

# Biomatrix from *Stipa tenacissima* L. and its Application in Fiberboard Using Date Palm Rachis as Filler

Mohamed Ammar<sup>1</sup>, Ramzi Khiari<sup>2,3,4\*</sup>, Mohamed Naceur Belgacem<sup>3,4\*</sup> and Elimame Elaloui<sup>1</sup>

<sup>1</sup>Materials, Environment and Energy Laboratory, Faculty of Sciences of Gafsa, University of Gafsa, Tunisia

<sup>2</sup>University of Monastir, Faculty of Sciences, UR13 ES 63 – Research Unity of Applied Chemistry & Environment, 5000 Monastir, Tunisia

<sup>3</sup>Grenoble Alpes University, LGP2, F-38000 Grenoble, France

<sup>4</sup>Grenoble Alpes University, CNRS, LGP2, F-38000 Grenoble, France

Received November 05, 2016; Accepted November 14, 2016

**ABSTRACT:** The present study investigated the preparation of biomatrices from *Stipa tenacissima* L. and its valorization for fiberboard application. Resins were produced by extracting lignin from the *Stipa tenacissima* L. black liquor by soda process and combining it with glyoxal as crosslinking agent to produce lignin-glyoxal-resin (LGR). The matrix was characterized by several methods, such as FTIR and ATG/ATD, and then mixed with date palm rachis as reinforcing fibers in different proportions of 30 and 50% (w/w with respect to the matrix) to produce biodegradable composite materials. Then, their thermal and mechanical properties were determined, using differential scanning calorimetry (DSC) and dynamic mechanical analysis (DMA). The results obtained show that date palm rachis particles were effective in enhancing the thermo-mechanical properties of the thermoset matrix.

**KEYWORDS:** Kraft lignin, thermosetting resins, date palm rachis, glyoxal, fiberboard, DMA

## 1 INTRODUCTION

Lignin, a natural, nontoxic polyaromatic polyol, is one of the most abundant and inexpensive sustainable polymers [1]. Standard and well-defined lignin is commercially available as a by-product of the paper-making industry. The annual global production of industrial lignin is reportedly around 50 million tons, which is almost 20% of the total production of industrial plastic [2]. However, the black liquor is treated mostly as a liquid waste and burnt to generate energy. Nevertheless, it is noteworthy that the presence of phenolic groups in lignin macromolecules makes lignin a potential macromolecular source to produce biopolymers or biomatrix. This finding was reported by several workers, namely, Ammar *et al.* [3], El Mansouri *et al.* [4], Alonso *et al.* [5] and others, who demonstrated that the use of formaldehyde as a crosslinking agent of lignin can produce promising matrices (LRF).

Moreover, many articles report that lignin-based phenol formaldehyde (LPF) resins can be used as binders for fiberboard [6], oriented strand board [7], plywood [8], etc. In fact, Wenjian *et al.* [9] suggest that lignin-phenol-formaldehyde resins can be used in the preparation of fiberboards [10]. Lei *et al.* succeeded in producing particleboard with good performance by substituting vegetable polyflavonoid tannins for LPF resin in adhesive formulations [6]. Currently, considerable attention is being paid to industrial development of natural, or green, wood adhesives such as soy protein-, tannin- and vegetable oils-based adhesives [7]. To this end, upgrading of aldehydes-free or hardeners-less tannin-based adhesives was started [6]. The development of polycondensation thermosets made of glyoxylated lignin (GL) and resorcinol was also reported [4, 6, 8, 11–14]. Following the same approach, lignin-glyoxal-resin (LGR) was prepared with the lignin extracted from *Stipa tenacissima* L. (using the kraft method), using glyoxal as a crosslinking agent. From a practical viewpoint, the rapid development in fiberboard production technology and the widespread use of fiberboard rendered these annual plant-based materials very useful, because non-wood plants need only 12 months for a full cycle of growth,

\*Corresponding authors: khiari\_ramzi2000@yahoo.fr; naceur.belgacem@pagora.grenoble-inp.fr

DOI: 10.7569/JRM.2016.634136

whereas trees require several years to grow. Non-wood plants and residues can also serve as substitutes for wood in the fiberboard industry, thus making valorization of annual plant wastes an intelligent practice.

Date palm is one of the most cultivated plants in southern Tunisia, which has more than 4 million plants occupying an area of about 32 thousand hectares, as reported in the Tunisian Ministry of Agriculture statistics [15]. This cultivation produces a huge amount of date palm rachis, which is left on the soil and allowed to biodegrade and thus fertilize the soil [16–18]. The date palm can be considered a potential raw material to produce fiberboard of composite material not only in Tunisia but also in all other countries where it abounds.

For this work, several composite films were prepared using a thermoset matrix LGR and incorporating date palm rachis fragment loadings in different proportions: 0%, 30% and 50%. The thermal and mechanical properties of the resulting sample were determined by differential scanning calorimetry (DSC), dynamic mechanical analysis (DMA) and tensile tests, following methods of the common standards.

## 2 EXPERIMENTAL

### 2.1 Date Palm Rachis

Date palm rachises from Gafsa (Tunisia) were collected, washed, rinsed with distilled water to eliminate sand and other soil contaminants and dried at room temperature for one month. The dried material was milled and sieved to a size of around 250  $\mu\text{m}$  and then successively extracted with ethanol-toluene before using.

### 2.2 Extraction of Lignin from Black Liquor

As described in our previous work [19], the isolated lignin was obtained from black liquor supplied by SNCPA, the National Society of Cellulose and Alfa Paper, using soda process (Kasserine, Tunisia). Briefly, the lignin (with pH = 12) was precipitated by adding sulfuric acid until the pH came down to 4.5. The precipitated lignin was washed with hot water (70 °C) for 30 min using a mechanical stirrer to remove residual sugar and adsorbed impurities. Then, the lignin was filtered and dried to a constant weight in an air circulation stove at 40 °C [19–21].

### 2.3 Resin-Lignin-Glyoxal Synthesis

The resin-lignin-glyoxal was prepared, under reflux, in a 6 dm<sup>3</sup> glass reactor equipped with a stirrer and a

condenser. Modified resins were synthesized following the method of El Mansouri *et al.* [4]. Samples, each weighing twenty grams of lignin, were prepared, to which glyoxal was added in the proportions of 30%, 40% and 50% (w/w with respect to lignin). In the meantime, 4.5 g of sodium hydroxide (based on dry weight) was added gradually in the form of 30 wt% aqueous solution and mixed for 45 min until the pH became 12 to 13. Then, the mixture was heated at 97 °C under a mechanical stirrer for 2 h and the solution cooled down to room temperature. The preparation of LGR resins was repeated at least three times.

### 2.4 Fiberboard Preparation

Fiberboards, measuring 350 × 300 × 14 mm, were prepared with date palm rachis and lignin-based matrix containing 50% of glyoxal (LGR<sub>50%</sub>) at a maximum pressure of 25 kg/cm<sup>2</sup> and a press temperature of 160 °C. A preliminary study was carried out in order to determine the optimal time and temperature. We have varied two parameters, the time from 10 to 30 min and the temperature from 160 °C to 200 °C. The best experimental conditions were established as: 20 min at 160 °C. The LGR composites reinforced with date palm rachis were prepared by mixing the thermoset matrix with lignocellulosic material at different loadings: 0, 30 and 50% (w/w with respect to the matrix). The total pressing time was maintained at 20 min.

### 2.5 Characterization of Resulting Materials

#### 2.5.1 FTIR Analysis

The resins were characterized using FTIR spectrophotometer (Bruker) by preparing KBr pellets with LGR concentration of 1% (w/w). The spectra were recorded between 600 and 4000 cm<sup>-1</sup> at a resolution of 4 cm<sup>-1</sup> and co-adding sixteen scans. To avoid pellet moisture contamination, the following procedure was followed: (i) resin fraction and KBr were left for 24 h at 40 °C under reduced pressure before pellet preparation; (ii) pellets were subjected to the same conditions for 12 h prior to FTIR analysis.

#### 2.5.2 UV Spectroscopy

Ultraviolet-visible (UV) spectroscopy offers a simple and rapid way of determining phenolic hydroxyl groups. The method is based on the difference in absorption between the lignins in alkaline, neutral and acid solutions [22]. For this purpose, 10 mg of the resin

was dissolved in 5 mL of dioxane and 5 mL of NaOH solution (0.2 mol/L<sup>-1</sup>). An aliquot of 2 mL of the prepared resin solution was diluted to 25 mL using buffer solutions of pH = 6 or 12, which yielded solutions with a final resin concentration of about 0.08 g.L<sup>-1</sup>. The UV spectra were recorded on a Shimadzu double-beam spectrophotometer, using the resin solution prepared at pH = 6 as the reference.

### 2.5.3 TGA Thermo-Degradation

Thermal gravimetric analysis (TGA; Perkin-Elmer Pyris 1 TGA-7) of fiberboard samples, each weighing about 15 mg, was carried out in a platinum sample pan, which was heated from 50 to 900 °C at a heating rate of 10 °C/min<sup>-1</sup> under nitrogen atmosphere with a flow rate of 20 mL/min<sup>-1</sup>. Curves of weight loss and derivative weight loss (DTG) were plotted [23]. The test was repeated at least twice.

### 2.5.4 Mechanical Properties

Dynamic mechanical thermal analysis (DMA) was performed using a DMA RSA III TA Instrument. A temperature range of 30 to 400 °C, at a heating rate of 3 °C/min<sup>-1</sup> and a frequency of 1 Hz, was applied after optimization of static and dynamic loads with a sample size of 16 × 10 × 1 mm. The measurements were repeated at least twice and the difference between the values obtained was within the experimental error of 5%.

The mechanical behavior of the fiberboard, which was cut into probe samples, each measuring 30 × 5 × 0.4 mm<sup>3</sup>, was evaluated by carrying out tensile and bending tests with a Rheometrics RSA 2 mechanical analyzer system, which works in tensile and bending modes. The elongation, stress at break, and Young's modulus were determined. All the samples were conditioned, as recommended by the ISO standard method, for 24 h in a conditioned room under a controlled temperature of 23 °C and relative humidity of 50%. These tests were performed five times and the difference between the values obtained was within the experimental error of 5%.

### 2.5.5 Internal Bond Test

All particleboards prepared from date palm and the LGR were tested for dry internal bond (IB) strength. This relevant test was conducted according to an international standard test; EN 314-1 (1993) and EN 314-2 (2004). It is a tensile test perpendicular to the plane of the board. The measurements were repeated at least five times and the difference between the obtained values was within the experimental error of 5%.

## 3 RESULTS AND DISCUSSION

### 3.1 Synthesis and Characterization of LGR

Three resins, namely LGR<sub>30%</sub>, LGR<sub>40%</sub> and LGR<sub>50%</sub>, were prepared with 30%, 40% and 50% of glyoxal respectively having pH of 12. From heating of these resins, it was noticed that the reactivity of the prepared resin depended on the proportion of glyoxal used. When the resins were heated to 80 °C, the gel time was 50 min for LGR<sub>30%</sub>, 39 min for LGR<sub>40%</sub> and 33 min for LGR<sub>50%</sub>, thus clearly indicating that the reactivity of LGR<sub>50%</sub> was the highest [9]. Figure 1, which presents the FTIR spectra of the prepared resins, shows the disappearance of the band at 1625 cm<sup>-1</sup> associated with the C=O of the glyoxal. The glyoxalization reaction is consistent with the FTIR spectra presented in Figure 1. The spectrum of raw lignin shows vibrations characteristic of guaiacyl and syringyl units: C–O at 1268 cm<sup>-1</sup>, C=O at 1214 cm<sup>-1</sup>, guaiacyl C–H and syringyl C–H at 1140 cm<sup>-1</sup> and C–H out-of-plane vibrations in positions 2, 5 and 6 of the guaiacyl units at 854 cm<sup>-1</sup> [21]. The intensity of these bands decreased or vanished in the spectrum of LGR<sub>50%</sub>, dried under subcritical conditions (1 day in air at room temperature, followed by 3 days in a ventilated oven at 105 °C). This finding indicates that guaiacyl units were indeed involved in condensation reactions with glyoxal.

Another feature worth mentioning is that the peak around 1710 cm<sup>-1</sup> in the lignin spectrum, attributed to C=O stretching of unconjugated ketones and carbonyl groups, is no longer visible in the spectrum corresponding to the resin network. This observation can suggest that aldehydes, initially present in lignin, might have contributed to its crosslinking.

The spectrum of the gel also showed absorption bands at 2919 and 2840 cm<sup>-1</sup>, associated with C–H stretching, and at 1462 cm<sup>-1</sup>, attributed to C–H deformation of methyl and methylene groups [22, 24].

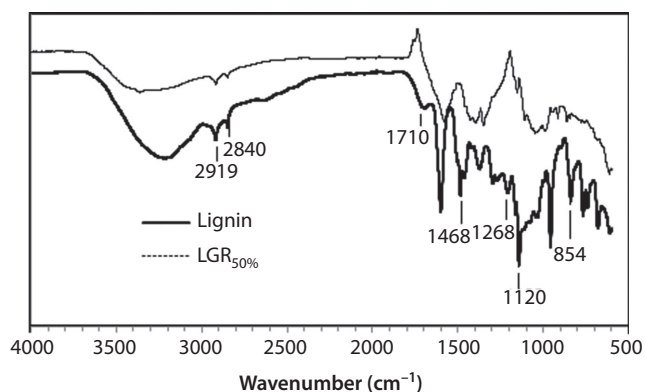


Figure 1 FTIR spectra of LGR<sub>30%</sub>, LGR<sub>40%</sub> and LGR<sub>50%</sub>.

Indeed, such groups participated in the formation of the three-dimensional crosslinked network structure of the gel.

UV-visible light absorption measurements were used for semi-quantitative assessment of the purity of lignin samples. The intensity of the absorbance is related to lignin concentration and is proportional to the purity of lignin. Therefore, as reported by Scalbert *et al.* [25], a lower absorbance was observed, indicating that modification of lignin had taken place. The main idea of this part is to follow up on the effect of glyoxal proportion on the crosslinking reaction.

Figure 2 presents the UV spectra of different samples of lignin: LGR<sub>30%</sub>, LGR<sub>40%</sub> and LGR<sub>50%</sub>. For all the samples, the maximum absorbance occurred at 280 nm, which was associated with the presence of non-conjugated phenolic groups in the lignin macromolecules. Interestingly, as shown in the spectra, the lowest absorbance values occurred in LGR<sub>50%</sub> samples, suggesting that these were the most crosslinked macromolecular fragments, as can be expected from the possible condensation reaction between glyoxal and the aromatic groups, as already deduced from gel-time determination. The amount of free phenolic hydroxyl groups in LGR is an important parameter because it conditions the reactivity of these groups and its effect on both chemical and physical properties of the lignin molecules. The total amount of ionized phenolic hydroxyl groups was calculated using the absorbance at 300 and 350 nm measured in 0.2 mol/L<sup>-1</sup> NaOH [26], and the results summarized in Table 1.

The UV-vis spectra (Figure 2) had three characteristic peaks, at about 250, 300 and 350–360 nm. The maxima at 250 and 300 nm are attributed to the absorbance

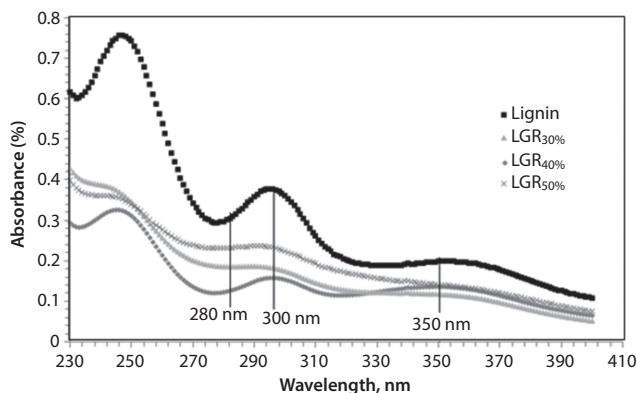


**Figure 2** UV spectra of lignin, LGR<sub>30%</sub>, LGR<sub>40%</sub> and LGR<sub>50%</sub>.

**Table 1** Quantification of hydroxyl groups I<sub>OH</sub>.

	Lignin	LGR <sub>30%</sub>	LGR <sub>40%</sub>	LGR <sub>50%</sub>
I <sub>OH</sub> mmol.g <sup>-1</sup>	1.131	0.478	0.545	0.702

of phenolate ions originated from unconjugated phenolic hydroxyl groups, whereas phenolic structures, conjugated with a carbonyl group, were absorbed at 250 and 350 nm [26]. From Table 1 it can be observed that the amount of free phenolic hydroxyl groups in LGR<sub>50%</sub> is lower than that in LGR<sub>30%</sub> and LGR<sub>40%</sub>, thus indicating that LGR<sub>50%</sub> is more reactive. The overall conclusion to be deduced from this observation is that LGR<sub>50%</sub> is the best one in terms of (i) gel time and (ii) UV spectra. For this reason, we decided to prepare our panel fiberboards with the LGR<sub>50%</sub>.

## 3.2 Preparation and Characterization of Fiberboard Panels

Several fiberboard panels (Figure 3) were prepared using fragments of date palm rachis (DPRF), and LGR<sub>50%</sub> as biomatrix. The thermal and mechanical properties of the prepared composites are presented and discussed below.

### 3.2.1 Thermogravimetric Analysis of Prepared Fiberboard Panels

Figure 4 shows the TGA curves for fiberboard panels prepared using date palm rachis in the proportions of 0%, 30% and 50%. These curves show four distinct zones of degradation: (i) the initial one appears nearly at 80–100 °C and corresponds to a small weight loss due to evaporation of absorbed moisture; (ii) the second event (at 230 °C) is associated with a sharp weight loss, which could be due to the water molecules produced during crosslinking reaction among methylol groups and/or with a freely positioned lignin aromatic ring; (iii) the third zone corresponds to the reaction of water and hydrogen with methylene group, which releases carbon monoxide and methane, respectively; (iv) the last zone (at 750 °C) corresponds to the ultimate charcoal thermal degradation.

Figure 4 clearly demonstrates that the addition of date palm rachis to LGR<sub>50%</sub>, as matrix, can enhance the stability of the prepared materials. Compared with the pure sample, the samples reinforced with date palm rachis showed a slightly lower kinetic of degradation, indicating higher thermal stability. This is due to higher and longer thermal resistance of the pyrolyzed lignocellulosic particles [16, 18]. Thus, when the temperature was increased, degradation occurred in several steps: (i) During the drying phase, i.e., when  $T < 200$  °C, the residual moisture was removed; (ii) When the temperature was between 350 and 400 °C, the hemicelluloses (the most thermally unstable compounds) underwent degradation. Beyond this temperature range, the slope of the curve changed, indicating a change in the chemical kinetics; (iii) When

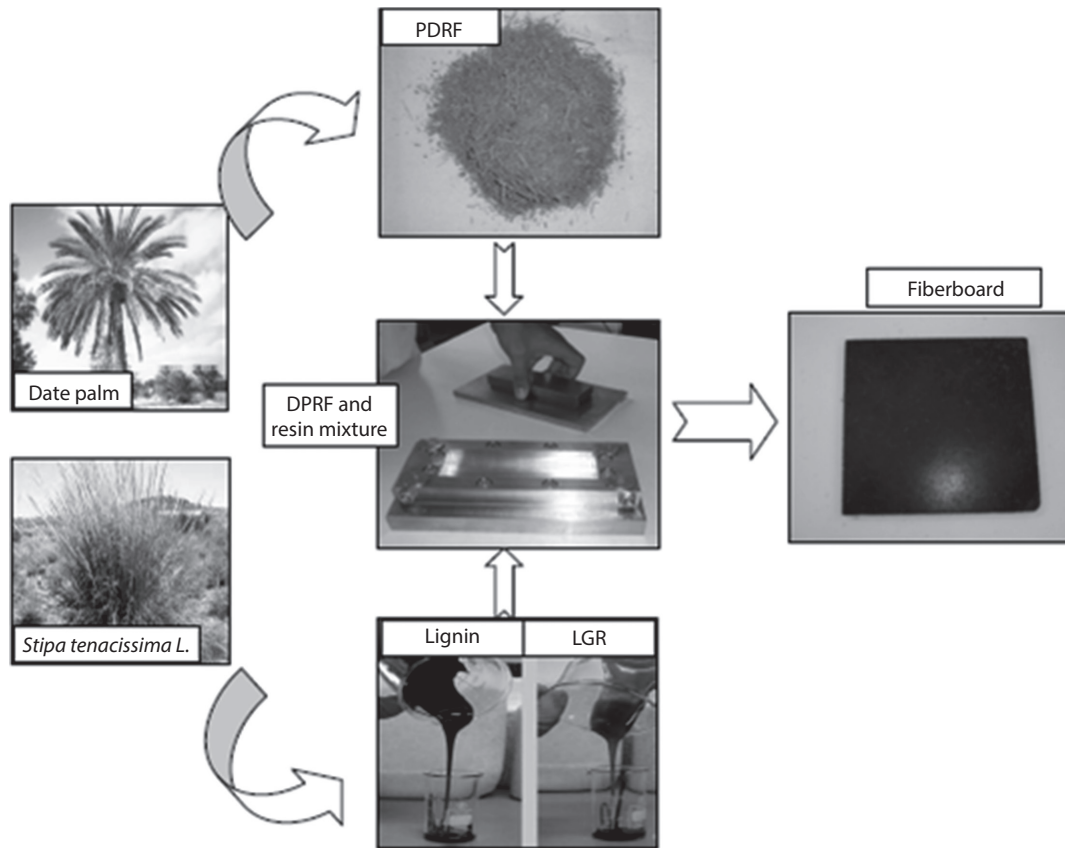


Figure 3 Fiberboard panels from rachis date palm and LGR<sub>50%</sub>.

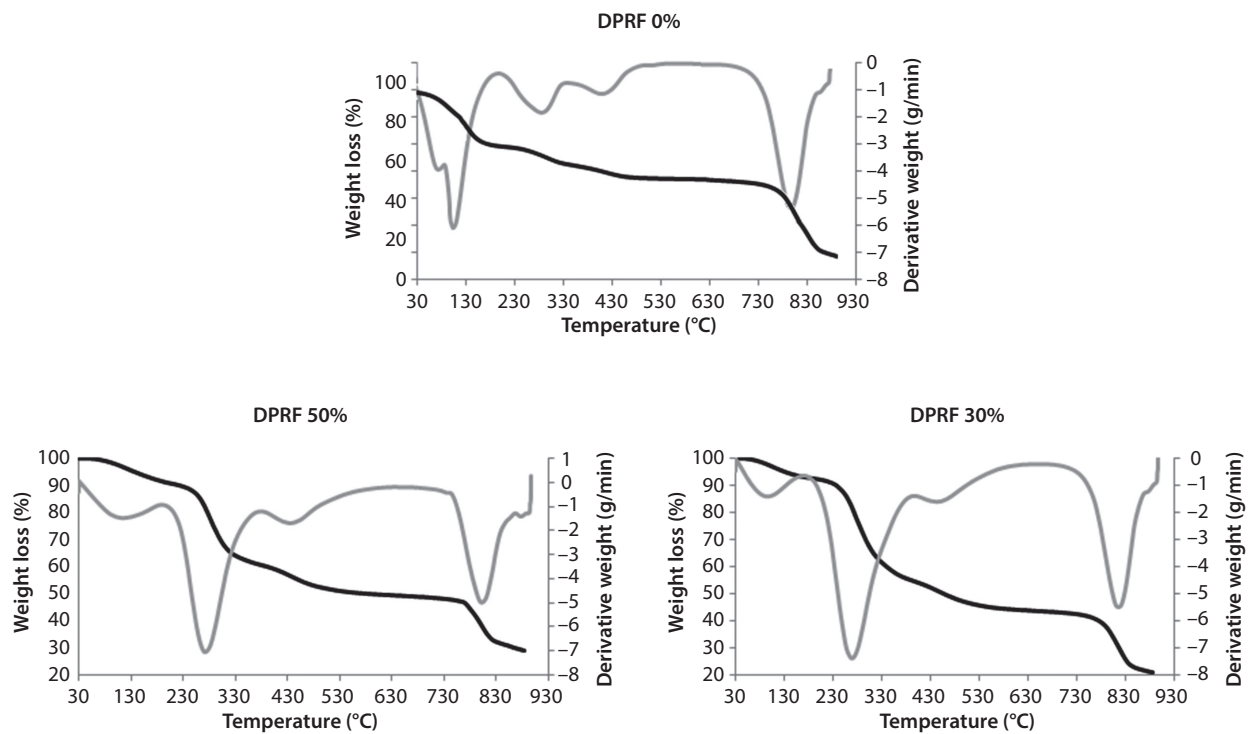


Figure 4 TGA and DTG curves of FB 0%, FB 30% and FB 50%.

the temperature was between 400 and 450 °C, degradation of residual lignin commenced; (iv) When the temperature exceeded 450 °C, ultimate degradation of lignin started and the kinetics of degradation became slower than that of the other compounds. However, it occurred over a wide temperature range, which rendered detection by ATG difficult.

### 3.2.2 Dynamic Mechanical Thermal Analysis

The mechanical tensile properties (Young's modulus, strength and elongation at break) were also investigated at room temperature (25 °C) and the results are summarized in (Table 2). As expected, the stress at break increased significantly as DPRF loading increased, because of the stiffening effect induced by lignocellulosic fillers; however, the elongation at break remained fairly unchanged (about 3%). Besides, the Young's modulus increased with an increase in filler's loading. For example, the Young's modulus of the composite, containing 50 wt% of DPRF, is more than three times that of the composite containing 30 wt% of DPRF. This confirms that the DPRF of date palm rachis plays a real reinforcing effect on the thermoset matrix (Table 2). This phenomenon can be attributed to the lignocellulosic added to the matrix, as previously reported for other cellulose fibers from other sources and other polymeric matrices [16, 18, 27].

Figure 5 shows the effect of DPRF loading on Young's modulus in the bending method of the prepared fiberboard. Generally, the optimum bending properties and Young's modulus are dictated by the volume of the reinforcing DPRF. Figure 5 shows that the Young's modulus increased significantly to 2.8 GPa as the added DPRF content was increased until 50 wt%. Then, the modulus started decreasing, probably because of insufficient filling of matrix resin and weak wettability between the matrix and the fibers [28]. Overall, the mechanical properties of the fiberboard, obtained by using our operating protocol, are significantly higher than those obtained by Dai and Fan, and close to those obtained by Amaral-Labat *et al.* [29, 30].

Dynamic mechanical thermal analysis, a means of studying the changes in the mechanical behavior of prepared composites as a function of temperature or frequency, is widely used to understand the effects of additives and fillers on composites or filled materials.

The plots of storage modulus and loss factor, as a function of temperature, for DPRF 30% and DPRF 50% are shown in Figure 6. The plots show that the addition of DPRF resulted in increasing the storage modulus of fiberboard, which reflects the reinforcement effect. For instance, DPRF 50% exhibits  $E'$  of 5 MPa relative to 2 MPa for DPRF 30%, indicating that adding 50% of fiber induced a more pronounced stiffening effect. Figure 6a shows the evolution of  $\tan(\delta)$  vs temperature at 1 Hz for different LGR composites. even if the values of  $T_g$  deduced from these graphs do not reflect the real phenomenon. Nevertheless, it retrieves a good idea of the transition temperatures for DPRF 30% and DPRF 50% (Table 3). It can be observed that DPRF 30% presented lower transition temperature ( $\alpha$  relaxation), compared to that presented by DPRF 50%, which can possibly be explained by lower interfacial adhesion, as discussed below.

Thus, interfacial adhesion is an important factor affecting the mechanical properties of polymer composites, as shown by the following equation [31]:

$$\frac{(\tan \delta_{\max})_B}{(\tan \delta_{\max})_m} = 1 - \beta\phi \quad (1)$$

Where:

- $(\tan \delta_{\max})_B$  and  $(\tan \delta_{\max})_m$  represent the weight of the  $\tan \delta$  peak of the blend and the polymer matrix in the DMA tests, respectively;
- $\phi$  is the volume fraction of the filler;
- $\beta$  refers to the interfacial adhesion parameter.

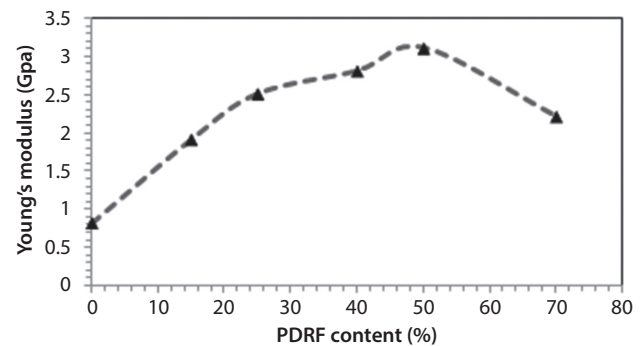


**Figure 5** Evolution of Young's modulus as a function of fiber content.

**Table 2** Mechanical tensile properties of composite films prepared with DPRF loadings (wt%).

	Young's modulus (MPa)	Stress at break (MPa)	Elongation at break (%)
DPRF 30%	0.29	0.66	3.0
DPRF 40%	0.56	1.7	2.9
DPRF 50%	1	3	2.3

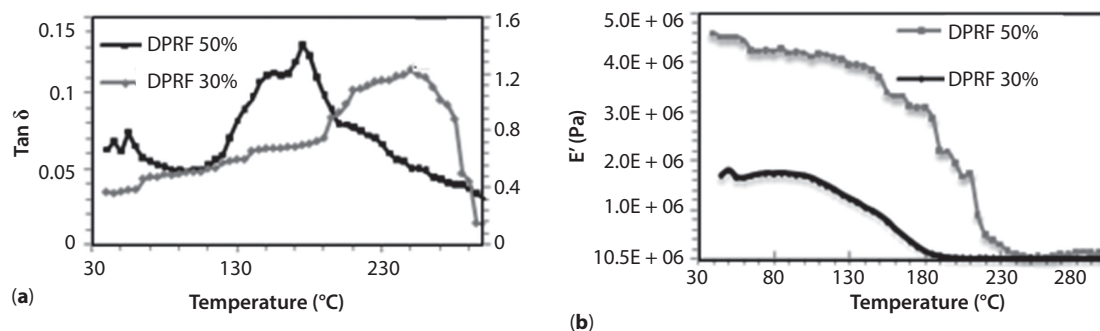


**Figure 6** Temperature dependence of loss factor  $\tan\delta$  (a) and storage modulus  $E'$  (b) of FB 30% and FB 50%.

**Table 3** Characteristics of DPRF 30% and DPRF 50%.

	$T_g(^{\circ}\text{C})$	$\phi$	$\beta$
DPRF 30%	175	0.58	0.22
DPRF 50%	240	0.38	0.02

It is generally considered that the larger the  $\beta$  value, the better would be the interfacial adhesion. Based on the densities of LGR and fibers,  $\phi$  can be obtained from mass fraction. After substituting the values of  $\phi$  and  $\beta$  in Table 3, it can be seen that, as expected, DPRF 30% shows the highest  $\beta$  value, i.e., 0.22, about ten times higher than the  $\beta$  value (about 0.02) of DPRF 50%. This implies that when the loading of DPRF is low, the cohesion is good, and consequently the interfacial adhesion with LGR matrix too; when the loading is high, the cohesion is usually poor. This explains the good thermal stability of DPRF 30%, as compared to that of DPRF 50%. Generally, the increase in fiber load enhances the mechanical property and decreases the thermal stability. This internal bond value was found to be 0.25 MPa. This value is higher than the requirement given by European standard EN314-2 and ANSI 2081, 1999 (0.1 MPa), for panels of this category [32] and it is in agreement with those obtained for similar commercial panels.

## 4 CONCLUSIONS

During this study, the effect of adding untreated particle fragments of date palm rachis, after milling and sieving, as reinforcing elements to cellulose-based composite materials, was investigated. First, a biomatrix from *Stipa tenacissima* L. was prepared by extracting lignin from the black liquor obtained after delignification of *Stipa tenacissima* L. and then glyoxal was added as a crosslinking agent, in different proportions, to produce lignin-glyoxal-resin (LGR). As discussed earlier, the best proportion of glyoxal was

found to be 50%, because the  $LGR_{50\%}$  thus obtained had the best reactivity. After that, different composites were successfully prepared with various amounts of 30 and 50 wt% of raw material (date palm rachis). The resulting materials were characterized for their thermal and mechanical properties. As expected, the TGA analysis demonstrated that the films reinforced with date palm fragments presented good thermal properties, which explain their stability and the shifting of temperature degradation. This work further demonstrated that the mechanical properties of the resulting samples were interesting, as borne out by the data obtained from Young's modulus. However, it must be mentioned that the results of water absorption properties stand out as negatives points.

## Acknowledgments

The authors express their thanks and sincere gratitude to "PHC-UTIQUE CMCU" as well as to IFC (Institut de Coopération Français de l'Ambassade de France en Tunisie, SSHN-2016) for their financial support.

## References

1. M.N. Belgacem and A. Gandini, *Monomers, Polymers and Composites from Renewable Resources*, Elsevier, Amsterdam (2008).
2. Q. Song, F. Wang, J. Cai, Y. Wang, J. Zhang, W. Yu, and J. Xu, Lignin depolymerization (LDP) in alcohol over nickel-based catalysts via a fragmentation-hydrogenolysis process. *Energy. Environ. Sci.* **6**, 994–1007 (2013).
3. M. Ammar, R. Khiari, M.N. Belgacem, and E. Elaloui, Isolation and characterization of lignin's from *Stipa tenacissima* L. and *Phoenix dactylifer*. *Cellulose Chem. Technol.* **48**, 255–263 (2014).
4. N.E. El Mansouri, A. Pizzi, and J. Salvado, Lignin-based polycondensation resins for wood adhesives. *J. Appl. Polym. Sci.* **103**, 1690–1699 (2007).
5. M.V. Alonso, M. Oliet, J. Garcia, F. Rodriguez, and J. Echeverria, Gelation and isoconversional kinetic

- analysis of lignin-phenol-formaldehyde resol resins cure. *Chem. Eng. J.* **122**, 159–166 (2006).
6. H. Lei, A. Pizzi, and G. Du, Environmentally friendly mixed tannin/lignin wood resins. *J. Appl. Polym. Sci.* **107**, 203–209 (2008).
  7. L. Lorenz, C.R. Frihart, and J.M. Wescott, in: *Proceedings of Wood Adhesives*, Forest Products Society, Madison, Wisconsin, pp. 501–506 (2006).
  8. M.A. Khan and S.M. Ashraf, Studies on thermal characterization of lignin substituted phenol formaldehyde resin as wood adhesives. *J. Therm. Anal.* **89**, 993–1000 (2007).
  9. Y. Wenjian, Q. Zhang, Z. Ye, and Z. Luo, Efficient statistical capacitance extraction of nanometer interconnects considering the on-chip line edge roughness. *Microelectron. Reliab.* **52**, 704–710 (2012).
  10. W. Hoareau, F.B. Oliveira, S. Grelier, B. Siegmund, E. Frollini, and A. Castellan, Fiberboards based on sugarcane bagasse lignin and fibers. *Macromol. Mater. Eng.* **291**, 829–839 (2006).
  11. P. Navarrete, A. Pizzi, S. Tapin-Lingua, B. Benjelloun-Mlayah, H. Pasch, K. Rode, L. Delmotte, and S. Rigolet, Low formaldehyde emitting biobased wood adhesives manufactured from mixtures of tannin and glyoxalated lignin. *J. Adh. Sci. Technol.* **26**, 1667–1684 (2012).
  12. P. Navarrete, A. Pizzi, H. Pasch, and L. Delmotte, Study on lignin-glyoxal reaction by MALDI-TOF and CP-MAS <sup>13</sup>C NMR. *J. Adh. Sci. Technol.* **26**, 1069–1082 (2012).
  13. F. Bertaud, S. Tapin-Lingua, A. Pizzi, P. Navarrete, and M. Petit-Conil, Development of green adhesives for fibreboard manufacturing, using tannins and lignin from pulp mill. *Cellulose Chem. Technol.* **46**, 449–455 (2012).
  14. P. Navarrete, A. Pizzi, K. Rode, M. Vignali, and H. Pasch, MALDI-TOF Study of oligomers distribution for stability-durable spray-dried glyoxalated lignin for wood adhesives. *J. Adh. Sci. Technol.* **27**, 586–597 (2013).
  15. R. Khiari, M.F. Mhenni, M.N. Belgacem, and E. Mauret, Chemical composition and pulping of date palm rachis and *Posidonia oceanica* – A comparison with other wood and non-wood fibre sources. *Bioresource Technol.* **101**, 775–780 (2010).
  16. R. Khiari, E. Mauret, M.N. Belgacem, and F. Mhenni, Tunisian date palm rachis used as an alternative source of fibres for papermaking applications. *Bioresources* **6**, 265–281 (2011).
  17. R. Khiari, Z. Marrakchi, M.N. Belgacem, E. Mauret, and F. Mhenni, New lignocellulosic fibres-reinforced composite materials: A stepforward in the valorisation of the *Posidonia oceanica* balls. *Compos. Sci. Technol.* **71**, 1867–1872 (2011).
  18. S. Mansouri, R. Khiari, F. Bettaieb, R.E. Abou-Zeid, F. Malek, and F. Mhenni, Characterization of composite materials based on LDPE loaded with agricultural Tunisian waste. *Poly. Comp.* **36**, 817–824 (2014).
  19. M. Ammar, R. Khiari, M.N. Belgacem, and E. Elaloui, Thermal characterization and comparisons of lignin-formaldehyde and lignin-glyoxal adhesives. *Med. J. Chem.* **2**, 731–737 (2014).
  20. S. Hattali, A. Benaboura, F. Ham-Pichavant, A. Nourmamode, and A. Castellan, Adding value to Alfa grass (*Stipa tenacissima* L.) soda lignin as phenolic resins (I). Lignin characterization. *Polym. Degrad. Stabil.* **75**, 259–264 (2002).
  21. R.C. Sun and J. Tomkinson, Fractional separation and physico-chemical analysis of lignins from black liquor of oil palm trunk fibre pulping. *Sep. Purif. Technol.* **24**, 529–539 (2001).
  22. A.A.M.A. Nada, M. El-Sakhawy, and S.M. Kamal, Infrared spectroscopic study of lignins. *Polym. Degrad. Stabil.* **60**, 247–251 (1998).
  23. J.M. Perez and A. Fernandez, Thermal stability and pyrolysis kinetics of lignin-phenol-formaldehyde resins. *J. Appl. Polym. Sci.* **123**, 3036–3045 (2012).
  24. W. Hoareau, G.T. Wanderson, B. Siegmund, A. Castellan, and E. Frollini, Sugar cane bagasse and curaua lignins oxidized by chlorine dioxide and reacted with furfuryl alcohol: Characterization and stability. *Polym. Degrad. Stabil.* **86**, 567–576 (2004).
  25. A. Scalbert, B. Monties, E. Guittet, and J.Y. Lallemand, Comparison of wheat straw lignin preparations – I. Chemical and spectroscopic characterizations. *Holzforchung* **40**, 119–127 (1986).
  26. G. Anna and G. Goran, Determination of phenolic hydroxyl groups in residual lignin using a modified UV-method. *Nord. Pulp. Paper. Res. J.* **14**, 163–170 (1999).
  27. A.K. Bledzki and J. Gassan, Composite reinforced with cellulose based fibers. *Prog. Polym. Sci.* **24**, 221–274 (1999).
  28. H. Akil and M.H. Zamri, Performance of natural fiber composites under dynamic loading. *Nat. Fibre Comp.* **2014**, 323–344 (2014).
  29. D. Dai and M. Fan, Wood fibres as reinforcements in natural fibre composites: Structure, properties, processing and applications. *Nat. Fibre Comp.* **2014**, 3–65 (2014).
  30. G.A. Amaral-Labat, A. Pizzi, A.R. Gonçalves, A. Celzard, S. Rigolet, and G.J.M. Rocha, Environment-friendly soy flour-based resins without formaldehyde. *J. Appl. Polym. Sci.* **108**, 624–632 (2008).
  31. M. Ashida, T. Noguchi, and S. Mashimo, Effect of matrix type on the dynamic properties for short fiber-elastomer composite. *J. Appl. Polym. Sci.* **30**, 1011–1021 (1985).
  32. T. Sellers, Jr., Wood adhesive innovations and applications in North America. XXI IUFRO World Congress in Kuala Lumpur, Malaysia, August 2000. *Forest Prod. J.* **51**(6), 12–22 (2001).